



Ultrafiltration fouling reduction with the pilot-scale application of ozone preceding coagulation, flocculation, and sedimentation for surface water treatment

Paul G. Biscardi, Steven J. Duranceau*

Department of Civil, Environmental, and Construction Engineering, University of Central Florida, 4000 Central Florida Blvd., Orlando, FL 32816-2450, USA, Tel. +1 407 823 1440; emails: paul@knights.ucf.edu (P.G. Biscardi), steven.duranceau@ucf.edu (S.J. Duranceau)

Received 13 March 2016; Accepted 13 April 2016

ABSTRACT

An ultrafiltration (UF) membrane process integrating ozone oxidation prior to a coagulation, flocculation, and sedimentation (CFS) pretreatment configuration processing surface water has been evaluated at the pilot-scale. Unlike prior research limited to short-term bench-scale evaluations, this current study provides information regarding the application of ozone oxidation prior to a CFS-UF pilot process operating over a four-month period (2,800 pilot runtime hours). In this work, changes in the long-term fouling behavior of the UF membrane process in response to the application of ozone prior to CFS pretreatment were characterized using fouling indices. When an average of 2.5 mg L^{-1} of ozone was applied prior to coagulation requiring 27 mg L^{-1} of polyaluminum chloride and a UF operating water flux of $85 \text{ L h}^{-1} \text{ m}^{-2}$, the chemically reversible and hydraulically irreversible fouling indices increased by 59 and 40%, respectively. A reduction of chemically irreversible fouling concomitant with a continuous improvement of normalized specific flux was observed over 1,240 pilot runtime hours of ozone application. The total fouling index decreased by 41% as compared to the baseline CFS-UF configuration. This research indicates that the use of ozone oxidation prior to a CFS-UF configuration can reduce membrane fouling when integrated with conventional surface water treatment.

Keywords: Ultrafiltration; Fouling indices; Membrane; Ozone; Coagulation

1. Introduction

Fouling is considered a major challenge faced during the operation of ultrafiltration (UF) membranes for surface water treatment. Pretreatment strategies to mitigate fouling and achieve enhanced removal can include both conventional treatment (coagulation, flocculation, and sedimentation, or CFS), and preoxidation

with ozone (preozonation). Preozonation, when applied under the appropriate conditions, has been shown to reduce downstream membrane fouling [1–3], and independently, act as a coagulant aid during conventional treatment [4,5]. However, few studies have investigated the use preozonation with pilot-scale membranes and less work has been published on the integration of both preozonation and CFS pretreatment prior to ultrafiltration.

*Corresponding author.

Bench-scale work has shown that preozonation can remove dissolved organic foulants such as humic substances that are known to cause chemically irreversible membrane fouling [6–8]. However, since most of this work has considered preozonation application directly ahead of the membrane process, work has been limited to ozone-tolerant ceramic membranes [9–12]. Also given the nature of bench-scale work, these studies were primarily short-duration tests.

While these bench-scale studies have provided insight into the possible mechanisms of fouling reduction by preozonation, very few pilot-scale studies have been published to assess the changes in long-term fouling behavior. Hashino et al. [3] tested an ozone-resistant polyvinylidene fluoride microfiltration membrane for treatment of surface water. In their pilot-scale work, ozone was applied directly ahead of the membrane process so that a residual of $0.3 \text{ mg L}^{-1} \text{ O}_3$ was detectable immediately upstream of the membrane surface. In this configuration, ozone was found to improve membrane permeability. Sartor et al. [13] evaluated preozonation of surface water prior to ultrafiltration followed by activated carbon filtration. This integrated hybrid process utilized a multi-channel flat sheet ceramic membrane which experienced less overall fouling compared to a control experiment without preozonation. Finally, Lehman and Liu [14] tested preozonation of wastewater in a pilot study of both ultrafiltration and microfiltration ceramic membranes. They demonstrated that preozonation was effective at removal of colloidal natural organic matter found in wastewater which subsequently led to reduced membrane fouling.

These pilot tests have further demonstrated the possible beneficial use of ozone and explored the mechanisms of how preozonation can reduce fouling. However, these studies have either been limited to ceramic membranes or have not considered integrating preozonation with conventional CFS processes. Furthermore, these studies did not quantitatively distinguish between hydraulically irreversible and chemically irreversible fouling. There are numerous examples of previous research that emphasizes the importance of distinguishing between the reversible and irreversible components of fouling [15–21]. Such a distinction is critical to assessing the long-term impact of incorporating preozonation with a membrane process and to further our understanding of the direct impact of preozonation on membrane foulants. As conventional water treatment plants continue to replace media filtration systems with membranes, the need for such information regarding fouling control using ozone has become increasingly important. Therefore, the purpose of this study was to

characterize changes in the fouling behavior of a polymeric UF membrane due to the implementation of preozonation in a CFS-UF process at the pilot-scale for treatment of surface water.

2. Experimental

2.1. Pilot study overview

The pilot study was conducted for approximately 4 months in northern California and utilized raw surface water from the South Bay Aqueduct (SBA). The SBA includes water from the Sacramento–San Joaquin Delta and, at times, surface water from Lake Del Valle. The average water quality characteristics observed during the pilot study are shown in Table 1. Water quality tests were conducted in accordance with standard methods [22].

The pilot study was conducted in three phases (or periods) to assess the impact of preozonation on membrane fouling behavior in a CFS-UF system. Since this study was one component of a larger pilot project, the initial runtime for Period 1 was 8,645 h as shown in Table 2.

Periods 1 and 2 represent a baseline for comparison with Period 3 when preozonation was applied. However, Period 2 is considered independently from Period 1 because during Period 2, a recycle stream was added to the pilot clarifier which returned backwash water from the UF pilot to the head of the treatment system. Table 2 also includes the number of data points recorded by the pilot and used during the fouling analysis. A diagram of the complete pilot process used in Period 3 is shown in Fig. 1.

2.2. Pilot-scale preozonation treatment system

The ozone pilot was a Wedeco MiPRO Advanced Oxidation Pilot System (Xylem Water Solutions, Charlotte, NC). The ozone pilot consisted of an ozone generator, controls, oxygen flow meter, oxygen flow control valve, ambient air ozone analyzer, sidestream injection system, four ozone contact chambers, an

Table 1
Average SBA water quality during pilot testing

Parameter	Average
Alkalinity (mg L^{-1} as CaCO_3)	77
Hardness (mg L^{-1} as CaCO_3)	94
Turbidity (NTU)	3.3
Total organic carbon (mg L^{-1})	6.5
Temperature ($^{\circ}\text{C}$)	16

Table 2
Description of pilot test periods

Period	Pilot runtime hours	Number of data points	Process configuration
1	8,645–9,626 (981 h)	28,774	CFS → UF
2	9,626–10,238 (612 h)	17,621	CFS → UF (with recycle)
3	10,238–11,477 (1,239 h)	35,132	Ozone → CFS → UF (with recycle)

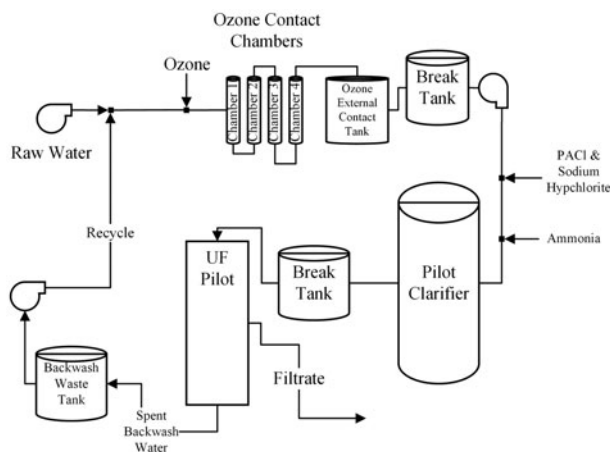


Fig. 1. Process flow diagram of the complete ozone–CFS–UF pilot system used during Period 3.

external ozone contact tank, dissolved ozone analyzer, and an off-gas and vent ozone concentration analyzer. To generate ozone, oxygen was concentrated from ambient air using a pressure swing adsorption system. An ozone generator then converted the concentrated oxygen into ozone. A main control panel was used to vary the oxygen feed rate and power to the ozone generator which in turn adjusted the ozone production rate. Ozone was injected into the raw water stream via an injector and sidestream pump. Contact time was provided by four 37-L vertical stainless steel contact chambers as well as one 1,100-L external vertical contact tank with a 0.9 m diameter. The ozone off-gas concentration from the contact chambers was monitored using an ozone analyzer fed from the top of each contact chamber and top of the external ozone contact tank. After detection, the off-gas from the contact chambers was sent to the ozone destruct unit.

The transferred ozone dose was typically maintained at 2.5 mg L^{-1} . However, for a two-week duration at the start of the test, the dose ranged from 1.8 to 2 mg L^{-1} . The dose was also adjusted when conducting calibration of the dissolved ozone analyzer. In this configuration, residual dissolved ozone was not detectable downstream of the final contact chamber during the pilot test.

2.3. Pilot-scale solid-contact clarifier

The pilot clarifier was a Westech Contact Clarifier Pilot (WesTech Engineering, Inc., Salt Lake City, UT). The flow through the pilot clarifier was set at 151 liters per minute. The clarifier feed water was dosed with polyaluminum chloride (PACI) between 25 and 30 mg L^{-1} to target a maximum turbidity of two nephelometric turbidity units (NTU) in the clarifier effluent. The clarifier feed water was also dosed with 5 mg L^{-1} sodium hypochlorite and ammonia at a 5:1 mass ratio (chlorine to ammonia ratio) based on free chlorine residual reading prior to the ammonia dosing.

2.4. Pilot-scale ultrafiltration membrane

The ultrafiltration pilot was designed and constructed by Harn R/O, Inc. (Venice, FL) and incorporated a Pentair X-Flow (Enschede, Netherlands) UF module. The pilot-scale hollow-fiber UF membrane was composed of a blend of polyethersulfone and polyvinylpyrrolidone and was operated in an inside-out, dead-end flow path configuration. The module contained a total of 15,000 fibers which made up a combined of 55 m^2 of total active area. Each fiber had a 0.8 mm diameter and was 1.5 m in total length. The nominal pore size of the membrane was $0.010 \mu\text{m}$ ($0.025 \mu\text{m}$ absolute) and the molecular weight cut-off was 200,000 Da. Over the course of the study, the UF pilot was operated at a constant filtration flux of $85 \text{ L h}^{-1} \text{ m}^{-2}$. UF pilot data were logged automatically in two-minute increments and included flow rates, filtration flux, transmembrane pressure (TMP), temperature, UF feed turbidity, UF filtrate turbidity, and cycle timers. Membrane integrity testing was performed manually to assess the membrane for fiber breaks twice a week.

Two cleaning regimes were used for the membrane including hydraulic backwashes with filtrate, and chemically enhanced backwashes (CEBs). The hydraulic backwashes were conducted every 45 min. During these backwashes, filtrate was flushed from the outside to the inside of the fibers. Each backwash was conducted at 227 liters per minute and lasted for 60 s. The CEBs were initiated every 24 h. Each CEB began

with a 10-min soak with 250 mg L⁻¹ sodium hypochlorite that was adjusted to a pH between 11 and 12 using caustic soda, and then was flushed with filtrate water at 227 liters per minute for 150 s to remove any chemical residual. Then, the CEB continued with a low-pH 10-min soak utilizing acetic acid with sodium bisulfite, mixed to a pH of 2–3 and then flushed with filtrate water at 227 liters per minute for 150 s to remove chemical residual.

During Periods 2 and 3, backwash waste from both the hydraulic backwashes and the CEBs was collected in a recycle tank. Recycled backwash water was pumped from this tank back to the influent raw water line at a rate of 6.8 liters per minute. This recycle stream achieved a 3% volumetric blend with the incoming raw water.

2.5. Analysis of pilot data

To quantify and distinguish between hydraulically and chemically irreversible fouling, data from this pilot test were first organized in terms of filtration sequence, CEB cycle, and study period using the data structure described by Boyd and Duranceau [23]. Fouling indices (FI) were subsequently calculated using the technique described by Nguyen et al. [18]. The fouling index was derived from the resistance-in-series model and can be described as follows:

$$\frac{1}{J'_s} = \frac{(J/\Delta P)_0}{(J/\Delta P)_V} = 1 + (FI)V \quad (1)$$

where J is the filtration flux (L h⁻¹ m⁻²), ΔP is the TMP (bar) corrected to 20°C, V is the specific permeate volume (L m⁻²), J'_s is the normalized specific flux (dimensionless), and FI is the fouling index (m⁻¹), which can be substituted with the total fouling index (TFI), hydraulically irreversible fouling index (HIFI), or the chemically irreversible fouling index (CIFI).

To determine these indices, raw two-minute data were collected regardless of the state of the pilot operation. Therefore, data collected near the beginning of a filtration sequence as the pump was ramping up, were often not representative of steady constant flux operation. To remove these data, outliers were detected and removed from raw data by identifying times when the flux set point had not yet been reached.

Then, the TFI, HIFI, and CIFI were each determined through linear regression of $1/J'_s$ plotted vs. specific volume. Only filtration sequences that contained between 20 and 22 data points were used to determine the TFI indices. For each of these filtration cycles, a linear regression of $1/J'_s$ data against specific

volume was conducted and the slope of each regression was taken to be the TFI. Then, the $1/J'_s$ data were averaged for each filtration sequence yielding 45-min averaged data. These filtration sequence averages were then grouped by CEB cycle. For each CEB cycle (containing at least 20 filtration cycles), a linear regression of the 45-min averaged filtration sequence $1/J'_s$ data against specific volume was conducted. The HIFI for a given CEB cycle was estimated as the slope of that linear regression. Finally, the $1/J'_s$ data from each CEB cycle was averaged and grouped by study period. For each study period, a linear regression of the averaged CEB cycle $1/J'_s$ data against specific volume was conducted. A linear regression of the average CEB cycle $1/J'_s$ data against specific volume was performed for each period and the slope of each regression was taken to be the CIFI. Average values of the hydraulically reversible fouling index (HRFI) and the chemically reversible fouling index (CRFI) as well as fouling index ratios were also calculated as described by Nguyen et al. [18].

3. Results and discussion

Daily averages of $1/J'_s$ are shown in Fig. 2. During Period 1, the $1/J'_s$ magnitude increased by approximately 30%. Most of this change occurred during the first half of Period 1 as $1/J'_s$ did not rise as rapidly during the second half. In Period 2, the $1/J'_s$ continued to rise and did not seem to be impacted by the implementation of a 3% recycle of ultrafiltration backwash water. However, when preozonation was applied during Period 3, the $1/J'_s$ decreased by approximately 28%.

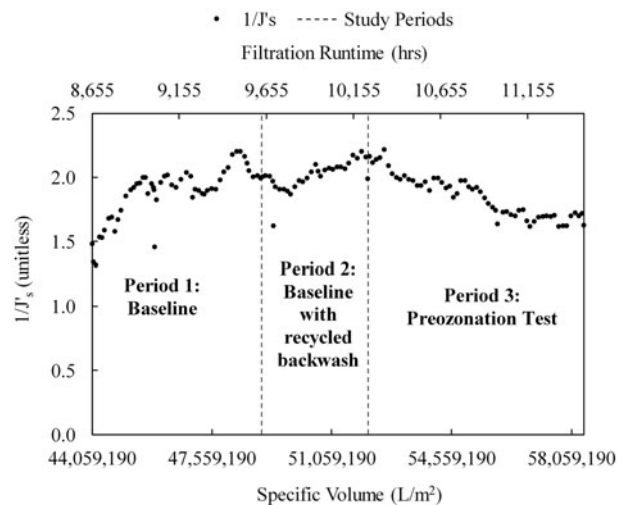


Fig. 2. Plot of $1/J'_s$ against specific volume for Periods 1–3.

Manual integrity testing suggested that no fiber breaks had occurred during the pilot test. This result agreed with total organic carbon (TOC) data displayed in Fig. 3 which showed no apparent change in the organic carbon removal by the UF pilot during Period 3 as well as Fig. 4 which showed no indication that filtrate turbidity had been compromised during Period 3.

To further understand the improvement in permeability during Period 3, the fouling behavior of the ultrafiltration pilot was analyzed by determining the TFI for each filtration cycle during Periods 1 through 3. These TFI values were then averaged by CEB cycle for visual clarity and plotted in Fig. 5. During Periods 1 and 2 the TFI increased as a function of specific volume. When preozonation was applied in Period 3, the TFI began to decrease and by the end of Period 3 the TFI had returned to conditions similar to those during the start of Period 1.

The HIFI data, shown in Fig. 6, revealed that the hydraulically irreversible fraction of the total fouling was slightly increased during Period 3 and therefore, did not explain the drop in TFI. An overall increase in HIFI had occurred throughout Periods 1–3. However, a plot of the HIFI/TFI index ratio shown in Fig. 7 revealed that the fraction of hydraulically irreversible fouling was higher in Period 3 compared to Periods 1 and 2.

The CIFI values for each period were determined and are presented in Fig. 8. During Period 3, the CIFI was $-8.1 \times 10^{-6} \text{ m}^{-1}$. The negative CIFI indicated that the membrane was experiencing a long-term “cleaning” trend whereby the CEBs were effectively restoring the membrane to increased permeability day-over-day. Likewise, the CRFI was $1.5 \times 10^{-6} \text{ m}^{-1}$

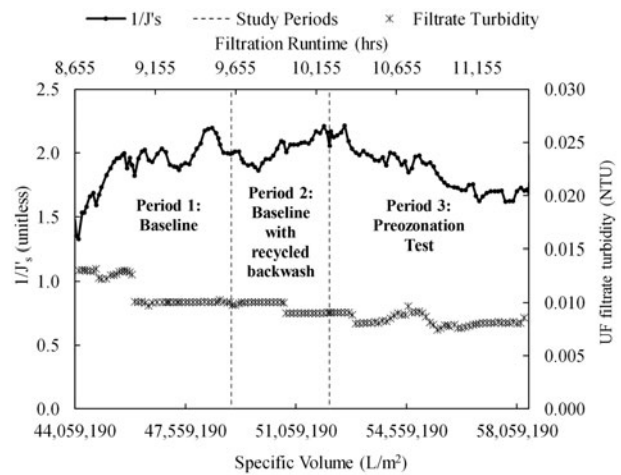


Fig. 4. Changes in filtrate turbidity during Periods 1–3.

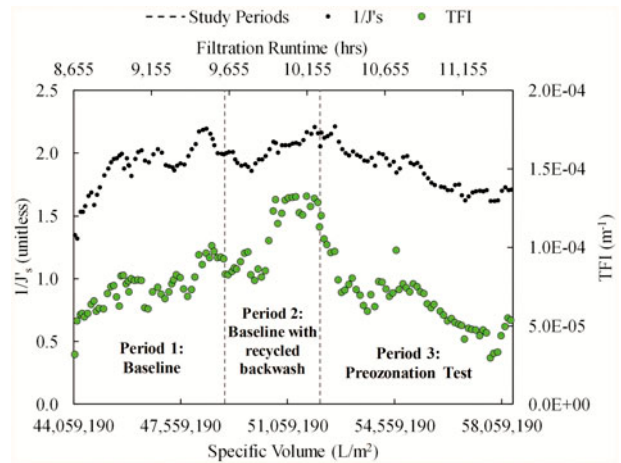


Fig. 5. Changes in TFI during Periods 1–3.

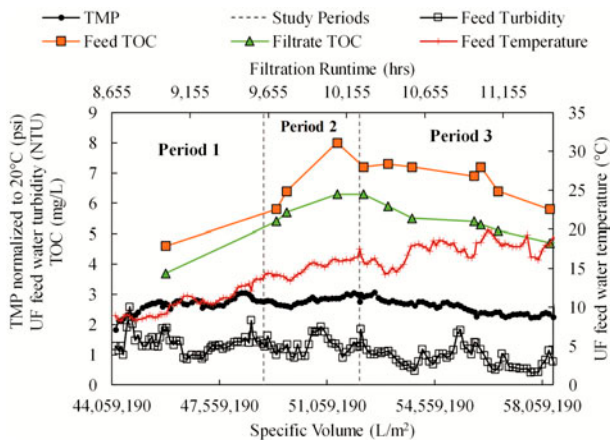


Fig. 3. TMP, TOC, feed temperature, and feed turbidity during study Periods 1–3.

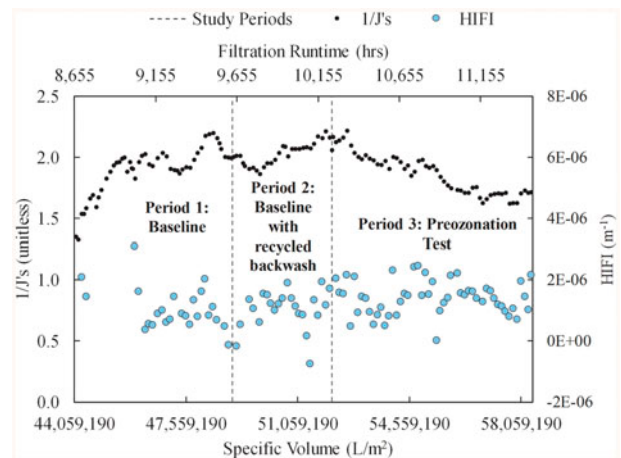


Fig. 6. Changes in HIFI during Periods 1–3.

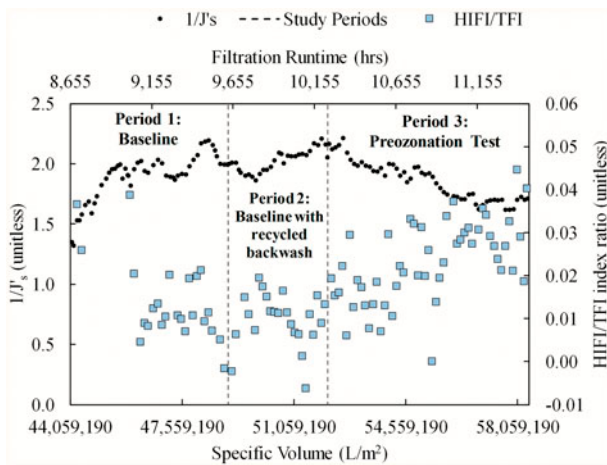


Fig. 7. Changes in HIFI/TFI ratios during Periods 1–3.

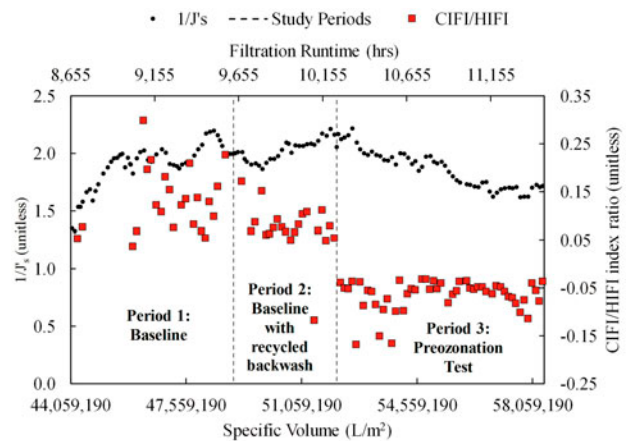


Fig. 9. Changes in CIFI/HIFI ratios during Periods 1–3.

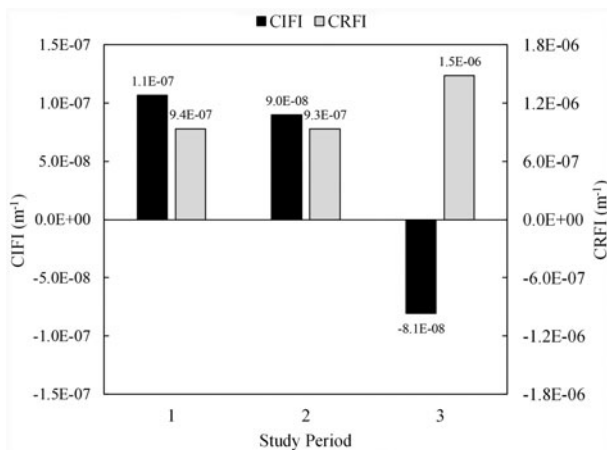


Fig. 8. Average CIFI for each period.

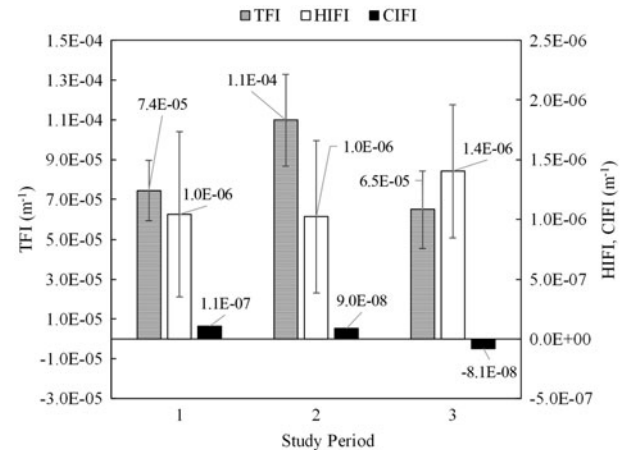


Fig. 10. Comparison of average TFI, HIFI, and CIFI for each period with error bars representing one standard deviation.

which represented a 59% increase in the chemical reversibility of the fouling experienced in Period 3 compared to Periods 1 and 2. This result suggested that the implementation of preozonation with CFS pretreatment had changed the characteristics of the foulants such that the fouling was now more chemically reversible than during Periods 1 and 2. Likewise, a plot of the CIFI/HIFI index ratio (Fig. 9) showed that the fraction of chemically irreversible fouling was lower in Period 3 compared to Periods 1 and 2.

Average fouling indices from Periods 1–3 are compared in Fig. 10. These results further indicated that preozonation changed the characteristics of the foulants such that the chemically enhanced backwashes became significantly improved. However, hydraulically irreversible fouling was higher during Period 3. These data suggest that the UF process could have

been further optimized by increasing the frequency of chemically enhanced backwashes when applying preozonation. Additional organic matter characterization may also aid optimization of the membrane process as this data may reveal the underlying changes to the organic foulants by ozonation which led to the improved chemical reversibility of the foulants.

4. Conclusions

The goal of this work was to investigate the effect of preozonation on the fouling behavior of an ultrafiltration membrane used to treat coagulated surface water at the pilot-scale. The major findings of this study are as follows:

- (1) Fouling indices revealed that membrane cleaning performance was affected by the implementation of preozonation.
- (2) TFI was reduced by 41% when preozonation was applied suggesting that the overall fouling rate had been reduced.
- (3) Preozonation led to improved chemically enhanced backwashes which increased CRFI by 59% and reduced chemically irreversible fouling.
- (4) Hydraulically irreversible fouling was increased when preozonation was applied as indicated by HIFI.

Acknowledgments

Funding for this project was provided by Harn R/O Systems (Venice, Florida) and the Alameda County Water District (Alameda County, CA) under UCF project agreement 16208088. This work was made possible through the tireless efforts of Steve Elola, Beth Gentry, Julie Harn, and Issam Najm. The authors are also grateful for the contributions of UCF students Shane Clark, Carlyn Higgins, Tiffany Miller, Michael Semago, and David Yonge.

List of symbols

J	—	filtration flux
ΔP	—	transmembrane pressure corrected to 20°C
V	—	specific permeate volume (cumulative volume of filtrate produced)
J'_s	—	normalized specific flux
TFI	—	total fouling index
HIFI	—	hydraulically irreversible fouling index
HRFI	—	hydraulically reversible fouling index
CIFI	—	chemically irreversible fouling index
CRFI	—	chemically reversible fouling index

References

- [1] Y. Song, B. Dong, N. Gao, S. Xia, Huangpu River water treatment by microfiltration with ozone pretreatment, *Desalination* 250 (2010) 71–75.
- [2] S. Lee, N. Jang, Y. Watanabe, Effect of residual ozone on membrane fouling reduction in ozone resisting microfiltration (MF) membrane system, *Water Sci. Technol.* 50 (2004) 287–292.
- [3] M. Hashino, Y. Mori, Y. Fujii, K. Nakatani, H. Hori, K. Takahashi, N. Motoyama, K. Mizuno, T. Minegishi, Advanced water treatment system using ozone and ozone resistant microfiltration module, *Water Supply* 1 (2001) 169–175.
- [4] P. Bose, D.A. Reckhow, The effect of ozonation on natural organic matter removal by alum coagulation, *Water Res.* 41 (2007) 1516–1524.
- [5] S. Sam, M.A. Yukselen, M. Zorba, J. Gregory, The effect of ozone on the reversibility of floc breakage: Suspensions with high humic acid content, *Ozone: Sci. Eng.* 32 (2010) 435–443.
- [6] R.H. Peiris, C. Hallé, H. Budman, C. Moresoli, S. Peldszus, P.M. Huck, R.L. Legge, Identifying fouling events in a membrane-based drinking water treatment process using principal component analysis of fluorescence excitation–emission matrices, *Water Res.* 44 (2010) 185–194.
- [7] K.L. Jones, C.R. O'Melia, Ultrafiltration of protein and humic substances: Effect of solution chemistry on fouling and flux decline, *J. Membr. Sci.* 193 (2001) 163–173.
- [8] C. Jucker, M.M. Clark, Adsorption of aquatic humic substances on hydrophobic ultrafiltration membranes, *J. Membr. Sci.* 97 (1994) 37–52.
- [9] W. Lee, H.-W. Lee, J.-S. Choi, H.J. Oh, Effects of transmembrane pressure and ozonation on the reduction of ceramic membrane fouling during water reclamation, *Desalin. Water Treat.* 52 (2013) 612–617.
- [10] J. Kim, S.H.R. Davies, M.J. Baumann, V.V. Tarabara, S.J. Masten, Effect of ozone dosage and hydrodynamic conditions on the permeate flux in a hybrid ozonation–ceramic ultrafiltration system treating natural waters, *J. Membr. Sci.* 311 (2008) 165–172.
- [11] B.S. Karnik, S.H.R. Davies, K.C. Chen, D.R. Jaglowski, M.J. Baumann, S.J. Masten, Effects of ozonation on the permeate flux of nanocrystalline ceramic membranes, *Water Res.* 39 (2005) 728–734.
- [12] B. Schlichter, V. Mavrov, H. Chmiel, Study of a hybrid process combining ozonation and microfiltration/ultrafiltration for drinking water production from surface water, *Desalination* 168 (2004) 307–317.
- [13] M. Sartor, B. Schlichter, H. Gatjal, V. Mavrov, Demonstration of a new hybrid process for the decentralised drinking and service water production from surface water in Thailand, *Desalination* 222 (2008) 528–540.
- [14] S.G. Lehman, L. Liu, Application of ceramic membranes with pre-ozonation for treatment of secondary wastewater effluent, *Water Res.* 43 (2009) 2020–2028.
- [15] H. Yamamura, K. Okimoto, K. Kimura, Y. Watanabe, Hydrophilic fraction of natural organic matter causing irreversible fouling of microfiltration and ultrafiltration membranes, *Water Res.* 54 (2014) 123–136.
- [16] K. Kimura, K. Tanaka, Y. Watanabe, Microfiltration of different surface waters with/without coagulation: Clear correlations between membrane fouling and hydrophilic biopolymers, *Water Res.* 49 (2014) 434–443.
- [17] R.H. Peiris, M. Jaklewicz, H. Budman, R.L. Legge, C. Moresoli, Assessing the role of feed water constituents in irreversible membrane fouling of pilot-scale ultrafiltration drinking water treatment systems, *Water Res.* 47 (2013) 3364–3374.
- [18] A.H. Nguyen, J.E. Tobiasson, K.J. Howe, Fouling indices for low pressure hollow fiber membrane performance assessment, *Water Res.* 45 (2011) 2627–2637.
- [19] J. Haberkamp, M. Ernst, H. Paar, D. Pallischeck, G. Amy, M. Jekel, Impact of organic fractions identified by SEC and fluorescence EEM on the hydraulic reversibility of ultrafiltration membrane fouling by secondary effluents, *Desalin. Water Treat.* 29 (2011) 73–86.

- [20] K. Kimura, T. Maeda, H. Yamamura, Y. Watanabe, Irreversible membrane fouling in microfiltration membranes filtering coagulated surface water, *J. Membr. Sci.* 320 (2008) 356–362.
- [21] D. Jermann, W. Pronk, S. Meylan, M. Boller, Interplay of different NOM fouling mechanisms during ultrafiltration for drinking water production, *Water Res.* 41 (2007) 1713–1722.
- [22] APHA, AWWA, WEF, *Standard Methods for the Examination of Water and Wastewater*, twenty-first ed., APHA-AWWA-WEF, Washington, DC, 2005.
- [23] C.C. Boyd, S.J. Duranceau, Evaluation of ultrafiltration process fouling using a novel transmembrane pressure (TMP) balance approach, *J. Membr. Sci.* 446 (2013) 456–464.